

Sources of H_0 -tension in dark energy scenariosBalakrishna S. Haridasu^{1,2,*}, Matteo Viel^{3,4,5,6,†} and Nicola Vittorio^{1,2,‡}¹*Dipartimento di Fisica, Università di Roma “Tor Vergata,” Via della Ricerca Scientifica 1, I-00133 Roma, Italy*²*Sezione INFN, Università di Roma “Tor Vergata,” Via della Ricerca Scientifica 1, I-00133 Roma, Italy*³*SISSA-International School for Advanced Studies, Via Bonomea 265, 34136 Trieste, Italy*⁴*INFN, Sezione di Trieste, Via Valerio 2, I-34127 Trieste, Italy*⁵*INAF-Osservatorio Astronomico di Trieste, Via Giovanni Battista Tiepolo 11, I-34143 Trieste, Italy*⁶*IFPU, Institute for Fundamental Physics of the Universe, via Beirut 2, 34151 Trieste, Italy*

(Received 29 December 2020; accepted 26 February 2021; published 29 March 2021)

By focusing on a simple extension of Lambda cold dark matter (Λ CDM) in which the dark energy equation of state is allowed to vary, we assess which epoch(s) possibly source the H_0 -tension. We consider cosmic microwave background (CMB) data in three possible ways: (i) complete CMB data; (ii) excluding the low- l + lowE ($l < 30$ temperature and polarization) likelihoods; (iii) imposing early Universe priors, which allow us to disentangle early- and late-time physics. Through a joint analysis with low-redshift supernovae type-Ia and gravitationally lensed time delay datasets, and neglecting galaxy clustering baryonic acoustic oscillation (BAO) data, we find that the inclusion of early Universe CMB priors is consistent with local estimate of H_0 , while excluding the low- l + lowE likelihoods mildly relaxes the tension. This is in contrast to joint analyses with the complete CMB data. Our simple implementation of contrasting the effect of different CMB priors on the H_0 estimate shows that the early Universe information from the CMB data when decoupled from late-time physics could be in agreement with a higher value of H_0 , even for Λ CDM model with no necessary modification. We also find no evidence for the early dark energy model using only the early Universe physics within the CMB data. Finally, using the BAO data in different redshift ranges to perform inverse distance ladder analysis, we find that the early Universe modifications, while perfectly capable of alleviating the H_0 -tension when including the BAO galaxy clustering data, would be at odds with the Ly- α BAO data due to the difference in r_d vs H_0 correlation between the two BAO datasets. We therefore infer and speculate that source for the H_0 -tension between CMB and local estimates could possibly originate in the modeling of late-time physics within the CMB analysis. This in turn recasts the H_0 -tension as an effect of late-time physics in CMB, instead of the current early-time CMB vs local late-time physics perspective.

DOI: [10.1103/PhysRevD.103.063539](https://doi.org/10.1103/PhysRevD.103.063539)

I. INTRODUCTION

The H_0 -tension is now significant at confidence levels $\gtrsim 5\sigma$ [1–5], making it the pressing issue to be resolved within the current/near-future cosmological scenario and possibly getting evidences for new physics beyond the standard Lambda cold dark matter (Λ CDM) model. Several proposals have been put forward attempting to resolve this tension, which can be classified based on the epoch(s) at which the modifications are suggested: high-redshift pre-recombination (early-time), low-redshift (late-time), and the local resolution. The early-time modifications [6,7] such as early dark energy [8–16], interacting dark energy [17–19], interacting dark matter [20,21], or early modified gravity [22],

among others [23–26] intend to modify the inferred scale of the sound horizon keeping the angular scales constrained by the cosmic microwave background (CMB) data [27] unchanged. Late-time modifications such as the decaying dark matter models [28–31] having prerecombination physics fixed to Λ CDM, which aim to increase the expansion rate at low redshifts and hence the H_0 , are also seemingly unable to relieve the tension [32–34] (see also [35]). Several attempts modifying the late-time phenomenology of the background expansion history also seem inadequate to relieve the tension [17,36–41]. On the other hand, the local resolutions [42,43] rely on correctly assessing the local “inhomogeneous” distribution of matter, essentially modifying the local estimate [43–45] to be in agreement with the lower high-redshift Λ CDM based H_0 . However, this approach is in contrast with the dynamics constrained by the Supernovae datasets [46–48], which do not allow sufficient variation in the local value necessary to

*haridasu@roma2.infn.it

†viel@sissa.it

‡nicola.vittorio@roma2.infn.it

completely resolve the tension and would also remain at a disadvantage to explain the higher values of H_0 obtained by the gravitational lensing time delay datasets [1,49–51]. See [52–58] for several extended discussions on possibilities of resolving H_0 -tension either contrasting different datasets and/or extensions to Λ CDM.

In this work we investigate the inferred H_0 value from the different components of CMB data, through selectively contrasting the CMB likelihoods with a combination of low-redshift data, using the simple one parameter extension allowing dark energy equation of state (EOS) $w \neq -1$ (w CDM). This extension was explored as a resolution to H_0 -tension where the EOS is required to be phantomlike ($w < -1$) [59–61], however with some nonstandard statistical interpretations. This model is clearly a low-redshift modification, as the dark energy component affects only the late-time evolution. By construction, this also allows us to make inferences for the $w = -1$, Λ CDM model. In the current work, we rely on a w CDM and an early dark energy model, owing to the fact that the $\Omega_k \neq 0$ extension is well known to be in even stronger discrepancy with the high values of the local estimate, having $H_0 \sim 55$ km/s/Mpc⁻¹ [27] and an even further discrepancy with baryon acoustic oscillations data, pointed out recently in [62,63]. However, as we discuss later in Sec. IV, our final inference would not depend on this choice.

We use the low-redshift Supernovae Type Ia (SN) [64] dataset which captures very well the dynamics of the background expansion and the gravitational lensing time delay (SL) [1,49] dataset, that complements the SN by providing constraints on H_0 , which is also in agreement with the local estimate. Incidentally, there is a good agreement in the H_0 vs w parameter space constraints obtained from the low-redshift SL [1,65] and high-redshift cosmic microwave background (CMB) [27] datasets, which is also a reason for the analyses performed here. It is also well known that the CMB based constraints on w are phantomlike at $\sim 95\%$ C.L. and in tentative tension with the Λ CDM model. In principle, one can find a three-way agreement between local model-independent SN based $H_0 = 73.48 \pm 1.42$ km/s/Mpc⁻¹ in Riess *et al.* [66] (hereafter R18), high-redshift CMB based $H_0 > 70.4$ km/s/Mpc⁻¹ (95% C.L.) [27], and low-redshift SL based $H_0 = 80.8_{-7.1}^{+5.3}$ km/s/Mpc⁻¹ [65] for a $w < -1$ dynamic dark energy extension. More recent estimates of the local $H_0 = 74.22 \pm 1.8$ km/s/Mpc⁻¹ [67] and $H_0 = 73.2 \pm 1.3$ km/s/Mpc⁻¹ [68] (hereafter R20) are available.

Traditionally, CMB based priors (reduced likelihood) have been through the distance, angular scales at the last scattering surface, the so-called shift parameters [69,70]. This implementation however remains model dependent for the extrapolated low-redshift behavior and need to be assessed separately for distinct cosmologies [71–73] (see Zhai *et al.* [74] for a more recent extended discussion).

In this context, we first conduct a “selective” contrasting analysis using a combination of high- l ($l \geq 30$) and CMB-lensing likelihoods from the latest Planck dataset, which is expected to minimize the effects of late-time physics [75]. Following which, we also use constraints obtained from this analysis as alternate priors, as proposed in Ref. [75] (earlier suggested in [76–78]), which intend to disentangle the late-time effects and obtain early-time priors from the CMB data, which are independent of standard model extensions such as the $w \neq -1$ and $\Omega_k \neq 0$, which affect the low-redshift evolution. Clearly, exclusion of data is not intended as a resolution of the H_0 -tension; however, the goal is to assess which epoch(s) within the CMB data gives rise to the tension with the local estimate and is in turn expected to possibly point towards desirable extensions/modifications of the current cosmological scenario. We also perform this analysis for the early dark energy model [8,79], which cannot, however, be interpreted as early Universe priors due to the specificity of the assumed model, but will help to assess the evidence for the model when utilizing only the early-time information in the CMB data.

In the main analysis, we do *not* include baryon acoustic oscillation (BAO) [80–83] datasets at low redshifts, as possible variations in the angular scales at high redshifts might be overlooked, which are well constrained by the CMB datasets and are necessarily assumed as fiducial cosmology, when obtaining the BAO observables. It is also well known that the BAO constraints on the dark energy EOS (w) are not in immediate agreement with the CMB based phantomlike inferences [84–87] and also that the BAO dataset based inverse distance ladder analyses mostly disfavor the late-time modifications [39,41,88,89]. However, see also relevant analyses made: (i) Ref. [90] (see also [91,92]), which claims an increased uncertainty of the BAO observables on the account of an assumed fiducial model through a purely geometric formalism; (ii) Ref. [93], where not assuming a CMB based fiducial cosmology shows increased uncertainty for varying dark energy EOS models (see Fig. 5 therein). These analyses suggest that the BAO observables might support a $w < -1$ scenario or a variation in the constraints of a $r_d \times H_0$ combination through increased uncertainties in the current observables. In effect, the mild disagreements between the constraints obtained from the isotropic and anisotropic components of BAO data reported in [85] might be pointing out for either underestimated uncertainty or an induced bias due to the assumed fiducial cosmology; all these efforts would require further investigation. However, we do rely on the BAO data to perform a simple inverse distance ladder analysis by assuming $\Omega_b h^2$ priors from the CMB data. This aids the discussion regarding the sufficiency of an early Universe modification to alleviate the H_0 -tension. Recently Ivanov *et al.* [79] and Hill *et al.* [94] (see also [95,96]) have argued that the early dark energy model is not adequate to alleviate the tension owing to no evidence with the CMB data alone

and discrepancy with large scale structure (LSS) data [97–100], respectively. However, see also [101–103]¹ where the LSS data is instead shown to be agreement with the EDE model.

The current paper is organized as follows: In Sec. II we describe the theoretical models implemented, followed by the description of the data in Sec. III. The results and discussions are presented in Sec. IV and finally we conclude in Sec. V.

II. THEORY AND MODELING

We test the flat ($\Omega_k = 0$) dynamical dark energy extension, with a constant EOS $w \neq -1$, for which the expansion rate is written as

$$\frac{H(a)^2}{H_0^2} \equiv E(a)^2 = \left[\frac{\Omega_r}{a^4} + \frac{\Omega_m}{a^3} + \Omega_{de} f(a) \right], \quad (1)$$

where $H(a)$ is the Hubble rate in terms of the scale factor a , $\Omega_i = \rho_i/\rho_{c0}$ is the current energy density of the i th component normalized to the current critical density of the Universe $\rho_{c0} = 3H_0^2 m_{pl}^2$ and subscript ‘0’ corresponds to the quantities measured today ($a = 1$). The time dependence of the dark energy component is modeled through the function $f(a)$ which can be written from the continuity equation as

$$f(a) = \exp \left[3 \int_a^1 \frac{d\tilde{a}}{\tilde{a}} (1 + w_\phi(\tilde{a})) \right], \quad (2)$$

which accounts to $a^{-3(1+w)}$ for a constant EOS, w CDM model. Distances are, as usual, estimated in the standard way for a flat background through the transverse comoving distance $D_M(z) = \frac{c}{H_0} \int_0^z \frac{d\tilde{z}}{E(\tilde{z})}$. Throughout the analysis we fix the radiation density² based on the usual implementation as in the Planck 2018 analysis [27].

Alongside the w CDM model we also perform minimal analysis for the early dark energy (EDE/3 pEDE) model.³ In this particular model, a light scalar field is conjectured that allows the effective cosmological constant to dynamically decay. The potential of the scalar field ϕ can be written as

$$V(\phi) = m^2 f^2 (1 - \cos(\phi/f))^n. \quad (3)$$

The physics of the scalar field can be described through effective field parameters z_c , $f_{\text{EDE}} = \rho_{\text{EDE}}(z_c)/3m_{pl}^2 H(z_c)^2$,

¹Note that the EDE modeling in [102] is different from that in [8,101].

²We assume the total radiation energy density as $\Omega_{r0} = 4.18343 \times 10^{-5}$, corresponding to the present $T_{\text{CMB}} = 2.7255 \text{ K}$ [104], which is the same implementation in Planck 2018 [27] analysis.

³We use the publicly available EDE modification of CLASS, CLASS_EDE provided by Hill *et al.* [94] at [105].

and $\theta_i = \phi_i/f$. Here z_c denotes the redshift at which the EDE contributes the most to the total energy density. Here we have kept the theoretical description of the EDE model to a minimum; please refer to Poulin *et al.* [8], Ivanov *et al.* [79], and Hill *et al.* [94] for an elaborate description of the theory and the modeling. Therefore, the effective dynamics of the scalar field will be described by three additional parameters: $\Theta_{\text{EDE}} \equiv \{f_{\text{EDE}}, \log_{10}(z_c), \theta_i\}$.

The transverse comoving distance D_M is related to the angular diameter distance $D_A(z) = D_M(z)/(1+z)$, which is used in the construction of the shift parameters:

$$R(z_*) = \frac{(1+z_*)D_A(z_*)\sqrt{\Omega_m H_0^2}}{c} \quad (4)$$

$$l_A(z_*) = \frac{\pi(1+z_*)D_A(z_*)}{r_s(z_*)} \quad (5)$$

where z_* is redshift to the photon decoupling epoch and r_s is the sound horizon. Also, when appropriate we use the numerical fitting formula for the sound horizon at drag epoch r_d , provided by Aubourg *et al.* [84].

III. DATA

A. Low-redshift probes

For low-redshift data we consider Supernovae Type Ia and strong lenses time delays.

1. Supernovae Type Ia

We use the pantheon compilation of 1048 supernovae (SNe) observations presented in [64] and have improved the statistical precision and the highest redshift ($z \sim 2$) to which the distances are measured. The likelihood for the SN dataset is implemented as suggested in the release [64].

2. Strong lenses

A combination of six gravitationally lensed time delay systems that were implemented earlier in [1,41] is considered. We follow the same procedure implemented in Wong *et al.* [1], closely replicating their results also in combination with the CMB datasets. The dataset implemented in Wong *et al.* [1] is an improvement over the four lenses dataset implemented earlier in Taubenberger *et al.* [65], with a corresponding improvement in the constraints on H_0 , reaching a 2.4% precision.

3. Baryon acoustic oscillations

We use a compilation of the angular diameter distance $D_A(z)/r_d$ and the Hubble rate $H(z) \times r_d$, at low redshift taken from [81] (DR12), at intermediate redshifts from [106] (DR14), and finally the high-redshift measurements of Ly- α forest, auto-correlation, and the Ly- α and quasars cross-correlation taken from [107,108] (Ly α 19), respectively.

TABLE I. Mean values and the corresponding covariances of the EUp-15 (early Universe priors from Planck15). H_{rec} and r_d are reported in Mpc^{-1} and Mpc , respectively.

| Observable | Mean | σ_i | r_{ij} | | | |
|--------------------|--------|-----------------------|----------|-------|-------|-------|
| $10^2\Omega_b h^2$ | 2.227 | 1.77×10^{-2} | 1. | -0.68 | -0.66 | 0.33 |
| $10^2\Omega_c h^2$ | 11.90 | 1.74×10^{-1} | -0.68 | 1. | 0.99 | -0.92 |
| H^{rec} | 5.188 | 2.44×10^{-2} | -0.66 | 0.99 | 1. | -0.93 |
| r_d | 147.49 | 0.36 | 0.33 | -0.92 | -0.93 | 1. |

B. High-redshift likelihood(s)

1. Early Universe priors

(EUp-15/EUp-18): Our goal is to disentangle the early-time constraints from the effects of the low-redshift behavior of models, as in [75] (hereafter V17). The constraints on the energy densities and expansion rate at the recombination era have been reported and shown to be independent of an additional degree of freedom, in particular w , Ω_k (cf. Table 2 therein). This is clearly evident of the well-expected fact that these components are much less dominant at the recombination epoch. These constraints were obtained with only the high- l ($l \geq 30$) and CMB-lensing [27] likelihoods and were appropriately reinterpreting the relevant parameters. The implemented prior is a combination of physical densities of cold dark matter, baryons, and the expansion rate at recombination H^{rec} and are summarized in Table I along with the covariances.⁴ The redshift of recombination in our analysis is effectively fixed to $z_{\text{rec}} = 1089.0$,⁵ as suggested in [75], given that the relative error is of the order $\sim 0.05\%$ and would yield no major difference to the inferred constraints. Originally, the authors of Ref. [75] have suggested the implementation of priors in the form of dimensionless matter densities at recombination $\{\Omega_b^{\text{rec}}, \Omega_c^{\text{rec}}, H^{\text{rec}}\}$; however, this also implies that the constraints on the physical densities $\{\Omega_b h^2, \Omega_c h^2\}$ ⁶ are essentially invariant, which we verify to be true across models and implement here as priors. These priors in fact are complementary to the Λ CDM model, as the necessary initial conditions at recombination and we choose this combination of data to quote our main inferences for the model. The inclusion of this early Universe CMB prior in the analysis is indicated as ‘‘EUp-15.’’ We replicate the analysis in Verde *et al.* [75] for which the covariance is reported in the Appendix A and elaborated in Sec. IV. Inclusion of the Planck 2018 early Universe priors are

⁴These covariances are constructed from the covariance matrix provided by Verde *et al.* [75].

⁵Note that we interchangeably use the notations z_{rec} and z_* , for ease of comparison with the earlier analysis, yet they are the same quantities.

⁶The physical densities are independent of the actual H_0 values as for the definition of critical density ($\rho_{c0} = 3H_0^2 m_{pl}^2$) used to obtain the dimensionless densities (Ω_i).

indicated in the analysis as ‘‘EUp-18.’’ We denote the analysis performed through this methodology using only the early-time information within the CMB data as ‘‘early Universe analysis’’ (EUA).

2. Reduced CMB likelihoods

(CMB/CMB [high- l]): We use the reduced CMB likelihoods through the distance priors simply by constructing the covariance among the observables $\{R(z_*), l_A(z_*), \Omega_b h^2\}$ [69,70]. Here we fix the redshift $z_* = 1089.79 \pm 0.26$ to its mean value, given the small value of the relative error $\sim 0.02\%$. We indeed verify that the inferences are equivalent and unchanged, when the z_* is either fixed or computed numerically, or even when utilizing the fitting formula from [109]. The uncertainty/covariance matrix for these observables was constructed utilizing the publicly available Planck chains⁷ for the w CDM cosmology, which we represent in the analysis simply as ‘‘CMB,’’ unless otherwise mentioned.

Additionally, we also implement a second reduced distance priors likelihood, in the spirit of the EUA, by first constraining the w CDM model utilizing only the high- l ($l \geq 30$) TTTEEE and the CMB-lensing likelihoods from the Planck 2018 release. Note that the aforementioned EUps are derived using the Planck 2015 likelihoods. Inclusion of these distance priors using only the high- l CMB likelihoods constraints is represented in the analysis as ‘‘CMB [high- l].’’ Constraints from this CMB analysis are presented in Sec. IV and reduced likelihoods for both these CMB dataset combinations are reported in Tables V and VI Appendix A. *A posteriori* we also conclude that the reduced likelihood estimated for the w CDM models performs equally well for the Λ CDM model in the joint analysis.

We implement the Bayesian analysis for the Planck likelihoods using the `MontePYTHON` package [77,110,111]. We use the `emcee` [112,113] package to perform the joint analysis of the low-redshift high-redshift likelihoods/priors. We then use the `getdist` [114] package [115] to analyze and infer posteriors from the chains. We also verify the comparison of the high-redshift observables between `CAMB` [116–118] based Planck chains and our runs which use the `CLASS` [119–121] code. For more details on the comparisons of `CLASS` vs `CAMB` implementations, please refer to [75,122]. Throughout the analysis we implement uniform, sufficiently wide flat priors on the Markov chain Monte Carlo (MCMC) parameters: $0.01 \leq \Omega_m \leq 0.5$, $50.0 \leq H_0 \leq 100.0$, $-2.5 \leq w \leq 0.5$. When including the CMB priors we use the priors of $0.01 \leq \Omega_{\text{cdm}} \leq 0.45$ and $0.02 \leq \Omega_b \leq 0.06$ on the energy densities of cold dark matter and baryons, respectively. For the additional

⁷We use the Planck w CDM chains obtained using the complete dataset combination of high- l + low- l + lowE + lensing denoted as ‘‘TTTEEE_lowl_lowE_post_lensing’’ in the publicly available chains.

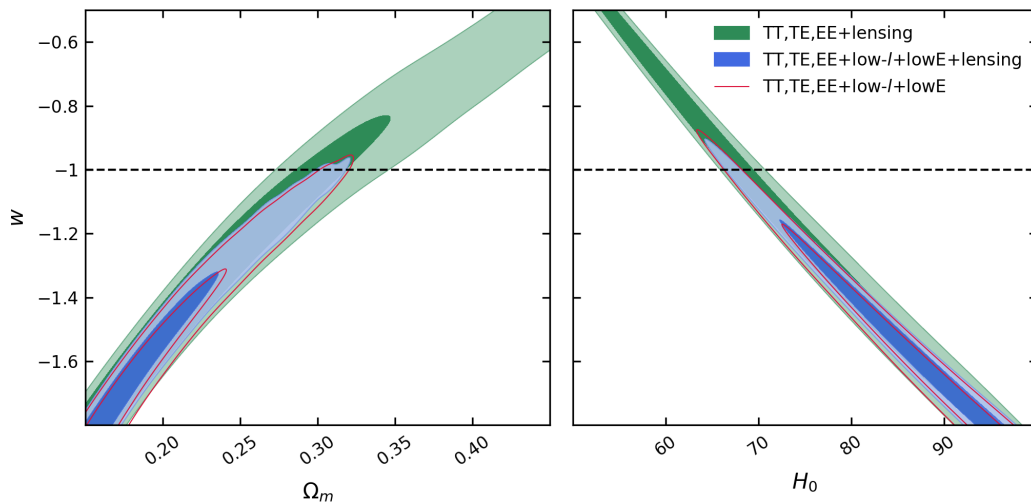


FIG. 1. Comparison of the Planck constraints for the w CDM model: in blue, the complete TT, TE, EE + low- l + lowE + lensing (CMB), in green the TT, TE, EE + lensing (CMB [high- l]) combination of likelihoods, and in red the combination of high- l + low- l + lowE are shown. H_0 is reported in the units of km/s Mpc^{-1} . The contours represent the 68% and 95% probability, respectively.

parameters of the EDE we implement the priors as were used in Hill *et al.* [94]: $0.001 \leq f_{\text{EDE}} \leq 0.5$, $3.1 \leq \log_{10}(z_c) \leq 4.3$, and $0.1 \leq \theta_i \leq 3.1$. Unless otherwise mentioned, we assess the MCMC analysis as converged with the Gelman-Rubin criteria [123] being at least $R-1 < 0.01$. Note that we sample on the effective parameters for the EDE model with uniform priors. Hill *et al.* [94] however show that implementing flat uniform priors on the physical parameters of the scalar field in fact provides tighter limits on the effective parameters, therefore having conservative final limits.

IV. RESULTS AND DISCUSSION

We begin by contrasting the CMB constraints on the w CDM model, all the Planck 2018 likelihoods and the high- l datasets alone, as described in Sec. III, essentially finding that the exclusion of the low multipoles relaxes the constraints on w and H_0 . As shown in the right panel of Fig. 1, the CMB constraints from the full dataset, which indicate much higher values⁸ of $H_0 > 82.4 \text{ km/s/Mpc}^{-1}$ at 68% C.L., are relaxed to $H_0 = 78_{-20}^{+10} \text{ km/s/Mpc}^{-1}$. At the same time, the phantomlike constraints of $w = -1.57_{-0.33}^{+0.16}$ from CMB are also relaxed to a $w = -1.30_{-0.54}^{+0.38}$ at 68% C.L. limits. One can also infer that the exclusion of the low- l + lowE likelihoods allow for a larger value of H_0 for the $w = -1$ (Λ CDM) parameter space from the same comparison in Fig. 1. In Table II, we report the constraints on the six base parameters and the additional EOS parameter w . Note the difference in reporting the parameter $100\theta_s$ in our analysis of CMB [high- l] to $100\theta_{\text{MC}}$

⁸Note that this w CDM based constraint on H_0 from Planck agrees with the local measurement of $H_0 = 73.48 \pm 1.42 \text{ km/s/Mpc}^{-1}$ reported in [66] within 2σ , owing to the 95% C.L. limit of $H_0 > 70.4 \text{ km/s/Mpc}^{-1}$.

in Planck CMB chains, due to varied implementation of the same from the CLASS to CAMB codes, respectively.

As expected, the constraints on the high-redshift behavior remain unchanged when excluding the low- l + lowE likelihoods. We find the sound horizon at the drag epoch to be $r_d = 147.29 \pm 0.32 \text{ Mpc}$ and $z_* = 1089.69 \pm 0.31$, which are practically equivalent to the constraints from the complete CMB dataset. This reasserts the “early Universe constraints” analysis in V17, at the same time hinting possible modifications of low- l modeling, which might aid in alleviating the H_0 -tension. The distance priors based reduced likelihood for CMB [high- l] constraints are presented in Appendix A. In summary, the major effect of excluding the low- l + lowE likelihoods is seen as degradation of the constraining ability of CMB data on the parameters of late-time physics (H_0, w), including the reionization optical (τ_{reio}) depth, which is, however, the least constrained parameter within the CMB analysis.

TABLE II. Comparison of the 68% C.L. limit constraints for the w CDM model from the complete CMB (second column) and with the exclusion of low- l + lowE (CMB [high- l]) likelihoods. In the last two rows, we show the derived* H_0 constraints in the units of km/s/Mpc^{-1} and σ_8 , respectively.

| Parameter | CMB [high- l] | CMB |
|---------------------------|---------------------------|---------------------------|
| $10^{-2}\omega_b$ | 2.247 ± 0.016 | 2.243 ± 0.015 |
| ω_{cdm} | 0.1188 ± 0.0015 | 0.1193 ± 0.0012 |
| $100\theta_{s/\text{MC}}$ | 1.04199 ± 0.00030 | 1.04099 ± 0.00031 |
| $\ln(10^{10}A_s)$ | $3.085_{-0.048}^{+0.032}$ | 3.038 ± 0.014 |
| n_s | 0.9673 ± 0.0052 | 0.9666 ± 0.0041 |
| τ_{reio} | $0.076_{-0.025}^{+0.018}$ | 0.0523 ± 0.0074 |
| w_0 | $-1.30_{-0.54}^{+0.38}$ | $-1.57_{-0.33}^{+0.16}$ |
| H_0^* | $78.0_{-20.0}^{+10.0}$ | > 82.4 |
| σ_8^* | 0.91 ± 0.11 | $0.964_{-0.044}^{+0.090}$ |

TABLE III. Constraints for the w CDM and EDE cosmological models using the CMB high- l (TT + TE + EE) and lensing likelihoods in the early Universe analysis. The reported constraints are 95% C.L. limits. Derived quantities are highlighted with a * superscript. The χ^2 improvement from w CDM to 3 pEDE is $\Delta\chi^2 \sim 1$, with $\chi^2_{w\text{CDM}} = 2355$.

| Parameter | $w\text{CDM}$ | EDE [$n = 3$] | |
|-----------------------|------------------------------|------------------------------|------------------------------|
| | | 3p | 1p |
| $10^{-2}\omega_b$ | $2.246^{+0.035}_{-0.035}$ | $2.260^{+0.043}_{-0.041}$ | $2.273^{+0.046}_{-0.044}$ |
| ω_{cdm} | $0.1190^{+0.0032}_{-0.0033}$ | $0.1211^{+0.0053}_{-0.0046}$ | $0.1216^{+0.0046}_{-0.0044}$ |
| $e^{-2\tau}A_s$ | $1.878^{+0.025}_{-0.024}$ | $1.882^{+0.030}_{-0.029}$ | $1.918^{+0.027}_{-0.024}$ |
| n_s | $0.966^{+0.011}_{-0.010}$ | $0.971^{+0.015}_{-0.014}$ | $0.976^{+0.015}_{-0.013}$ |
| w_{fld}^0 | $-1.27^{+0.72}_{-0.69}$ | ... | ... |
| $\log_{10}(z_c)$ | ... | $3.72^{+0.56}_{-0.45}$ | ... |
| f_{EDE} | ... | <0.071 | <0.080 |
| θ_i | ... | $2.0^{+1.1}_{-1.7}$ | ... |
| z_{rec}^* | $1088.96^{+0.65}_{-0.71}$ | $1089.02^{+0.67}_{-0.65}$ | $1088.89^{+0.66}_{-0.60}$ |
| r_{d}^* | $147.24^{+0.63}_{-0.63}$ | $145.9^{+1.7}_{-2.6}$ | $145.5^{+2.0}_{-2.3}$ |

The values of the reionization optical depth are pushed towards higher values $\tau_{\text{reio}} = 0.076^{+0.018}_{-0.025}$ with larger uncertainty, yet in agreement with the tight constraint of $\tau_{\text{reio}} = 0.059 \pm 0.006$, reported in Pagano *et al.* [124], within standard analysis.

We replicate the analysis performed in V17, which essentially excludes the low- l + lowE likelihoods and marginalizes over the amplitude and tilt parameters of the Newtonian lensing potential [see Eq. (4.1) in V17],⁹ which are now additional parameters of the MCMC analysis. As implemented in V17, the reionization optical depth is fixed to $\tau = 0.01$, owing to the degeneracy with the parameter amplitude of the scalar fluctuations A_s . The results for ΛCDM analysis are shown in Table III. In this scenario, the extrapolated H_0 is not interpreted as the current expansion rate, but rather fixes the distance to the last scattering surface. Note that in Fig. 7 (Appendix A), we show the comparison of the constraints on the matter density and expansion rate at recombination between the Planck 2015 analysis in V17 and our Planck 2018 analysis, finding no major difference. The mild differences are within the correlations between the physical densities and a small shift in the constraint on ω_b , as shown in Table VII.

In this context we also perform the early Universe analysis of V17, as described above, with the EDE model (shown in the last two columns of Table III). Using the same CMB data along with the additional three EDE parameters (Θ_{EDE}) we assess the evidence for the EDE model. We find a limit of $f_{\text{EDE}} < 0.07$ at 95% C.L., which is similar to the limits of $f_{\text{EDE}} < 0.06$ [94] and $f_{\text{EDE}} < 0.07$

in [95] found with the complete CMB data and additional low-redshift large scale structure data, without the inclusion of local H_0 . In fact, our 95% C.L. from the EUA is slightly tighter than $f_{\text{EDE}} < 0.087$ obtained from complete CMB data alone. Our limit from the EUA is also equivalent to the limits found in Ref. [94] with the complete CMB data, BAO, SN, and full shape analysis of the BOSS power spectrum. This essentially indicates that there is even weaker evidence for the EDE modification, when assessing it only against the early-time information in the CMB data. Also, the χ^2 improvement is of the order of $\Delta\chi^2 \sim -1.0$ ($\chi^2_{\text{EDE}} = 2354$) for the EDE modification. In Hill *et al.* [94], it was reported that the χ^2 for the high- l (TT+TE+EE) dataset becomes worse with the EDE modification by $\Delta\chi^2 \sim 2.6$, when including the local H_0 value (please see Table VII of [94]) in the joint analysis. Also, this indicates that the early-time physics within the CMB data does not support the current early dark energy extension to ΛCDM . However, note that more recently in Ref. [101], it has been shown that fixing the $\{\log_{10}(z_c), \theta_i\}$ parameters considerably increases the allowed range for the f_{EDE} parameter (1 pEDE) while having the same χ^2 value. This implementation appropriately implies a fine-tuned early Universe allowing us to sample better the f_{EDE} parameter space, which, in a MCMC analysis, tends to collapse the posterior distribution on the ΛCDM model ($f_{\text{EDE}} \sim 0$). A similar inference was also made in Ref. [26] for acoustic dark energy and in Ref. [22] for early modified gravity models. This highlights the dependence of the posteriors on the choice of priors, elaborated in Ref. [125]. Within the EUA we find the best-fit values of $\{\log_{10}(z_c), \theta_i, f_{\text{EDE}}\} = \{3.89, 2.74, 0.035\}$, which for the former two parameters are similar to values from the full CMB analysis [94,101,125]. The f_{EDE} , however, has a lower best-fit value, in comparison to the 0.068 in Ref. [94] and 0.085 in Ref. [125]. We infer these differences as the effect of the late-time information within CMB data also for the EDE model. Although the limits obtained in our analysis are tighter, in agreement with Ref. [125], we also find that our best-fit f_{EDE} value is different from the peak of the posterior and close to the 1σ bounds.

We stress that one should interpret the strengthening of the limits, obtained with the exclusion of late-time physics in the EUA analysis, as a shift in the confidence regions, however, sharply bounded on the lower end, which gives the impression of tighter limits. Tables VII–X in [125] show that in the 1 pEDE formalism and/or the inclusion of the local H_0 , yielding higher values of f_{EDE} always worsens the fit to the high- l likelihood. This validates our tighter limits (lower values) on the f_{EDE} parameter, which is obtained using only the high- l information, while having a mild preference for the EDE over the ΛCDM model. From the χ^2 comparison, noticing that higher values of f_{EDE} imply better fit to low- l and worse fit to high- l likelihoods, we expect that the 1 pEDE with the EUA lacking the low- l pull might not be

⁹Please refer to Vonlanthen *et al.* [76] and Audren *et al.* [77] for earlier discussions on the procedure to disentangle the late-time effects and the early Universe physics in the CMB analysis.

able to relax the bounds on f_{EDE} . To validate the same, we perform the EUA with the 1 pEDE model, wherein we fix the $\{\log_{10}(z_c), \theta_i\}$ parameters to their best fit from the 3 pEDE analysis. We find that the mean of the posterior now shifts to be in better agreement with the best fit of f_{EDE} from the 3 pEDE analysis. The 95% upper limit also increases mildly to <0.08 with a 65% C.L. constraint of $f_{\text{EDE}} = 0.038^{+0.015}_{-0.031}$.

In addition to the points made above, Ref. [101] shows that lower values of A_s obtained from the LSS observations, in comparison to the CMB constraints, lead to the discrepancy claimed by [79]. Within our EUA, we do not have constraints on the A_s parameter alone but only for the combination parameter $e^{-2\tau}A_s$. We find that the quantity $e^{-2\tau}A_s$ is almost equivalent for both the models and is also compatible with the Λ CDM constraints obtained from the full data [27]. In Fig. 2, we show the comparison of the constraints on H_0 and σ_8 in the EUA for the two models. We stress that in the EUA there exists no interpretation of

H_0 and σ_8 , which are parameters constraining late-time physics. However, the strong positive correlation between the H_0 and σ_8 shows why a simple dark energy extension of $w \neq -1$ is inadequate to resolve the H_0 -tension. Higher values of H_0 that imply higher values of σ_8 will be in significant tension with the lower valued σ_8 constraints from the LSS [97,126–129] data. Note that the tension is usually represented in terms of the compound parameter $S_8 = \sigma_8 \sqrt{\Omega_m/0.3}$ [130] and the arguments for tension would be equivalently valid and enhanced if σ_8 and Ω_m are positively correlated.

We now proceed to perform the joint analysis of the low-redshift SN and SL datasets in conjunction with the CMB/EUp priors as described in Sec. III and reported earlier in this section. In Table IV, we show the constraints for the w CDM model parameters and the corresponding contours in Fig. 3. As it can be seen, the first two rows are in very good agreement with those quoted in Wong *et al.* [1],

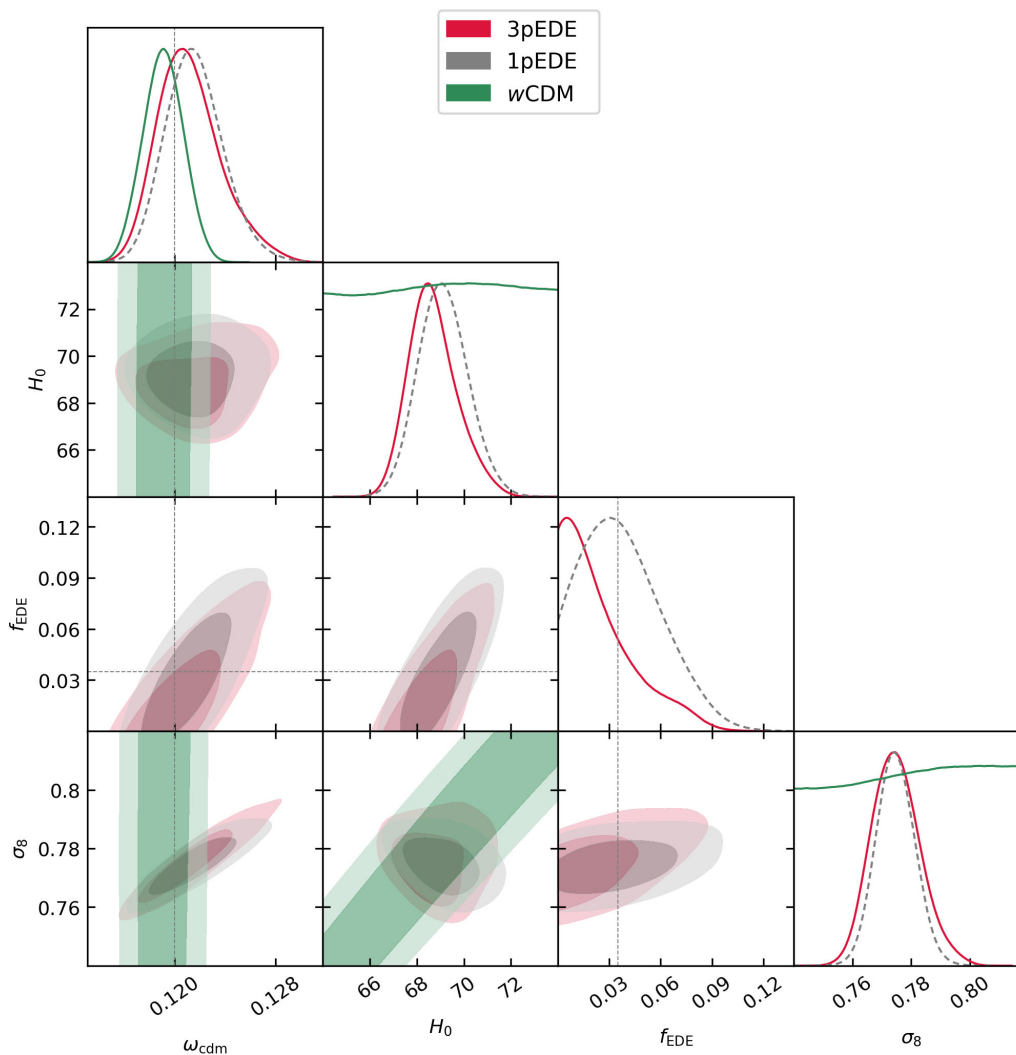


FIG. 2. EUA comparison of the w CDM model and the EDE model. The 3 pEDE 95% C.L. limits correspond to $f_{\text{EDE}} < 0.07$. The 3 pEDE and 1 pEDE analysis have the convergence criteria of $R - 1 \lesssim 0.08$ and $R - 1 \lesssim 0.01$, respectively. The dashed markers show the best-fit values of the f_{EDE} and ω_{cdm} parameters in the 3pEDE model.

TABLE IV. Constraints on the w CDM model at 68% confidence level obtained for various combinations of datasets. We quote the maximum posterior and the 16th, 84th percentiles as the uncertainty^a.

| Parameter Data | Ω_m | w | H_0 [km/s Mpc ⁻¹] |
|----------------------------|---------------------------|----------------------------|---------------------------------|
| SL | $0.30^{+0.13}_{-0.10}$ | $-2.32^{+0.77}_{-0.17}$ | $81.4^{+5.3}_{-5.0}$ |
| SL + CMB | $0.236^{+0.022}_{-0.016}$ | $-1.315^{+0.111}_{-0.091}$ | $77.6^{+2.7}_{-3.4}$ |
| SL + SN | $0.361^{+0.056}_{-0.068}$ | $-1.13^{+0.19}_{-0.24}$ | $75.1^{+2.2}_{-2.5}$ |
| SL + SN + EUp-15 | $0.266^{+0.014}_{-0.010}$ | $-0.929^{+0.045}_{-0.057}$ | $72.5^{+1.7}_{-1.5}$ |
| SL + SN + EUp-18 | $0.268^{+0.012}_{-0.013}$ | $-0.939^{+0.049}_{-0.050}$ | $72.5^{+1.7}_{-1.6}$ |
| SL + SN + CMB | $0.296^{+0.009}_{-0.010}$ | $-1.046^{+0.032}_{-0.040}$ | $69.5^{+1.1}_{-1.0}$ |
| SL + SN + CMB [high- l] | $0.288^{+0.012}_{-0.009}$ | $-1.032^{+0.039}_{-0.035}$ | $69.6^{+1.2}_{-1.0}$ |

^aWe quote the maximum posterior values instead of the mean, as it captures the nature of skewed distributions better.

except for mild differences in the posteriors. We also implement slightly different uniform priors on the parameters as reported in Sec. III, with no consequence for the inferred posteriors. Considering the dataset SL + SN + CMB for the w CDM model, the posterior on H_0 is driven towards lower values, due to the almost orthogonal correlations in the Ω_m vs w plane of the CMB and SN + SL datasets. Replacing the CMB distance priors with CMB [high- l] priors induces a parallel shift (keeping the correlation intact) in the contours towards $w > -1$ and mildly higher values of H_0 . The variation in the CMB constraints shown in Fig. 1 with the exclusion of low- l + lowE datasets does not weigh enough to modify the H_0 estimates within

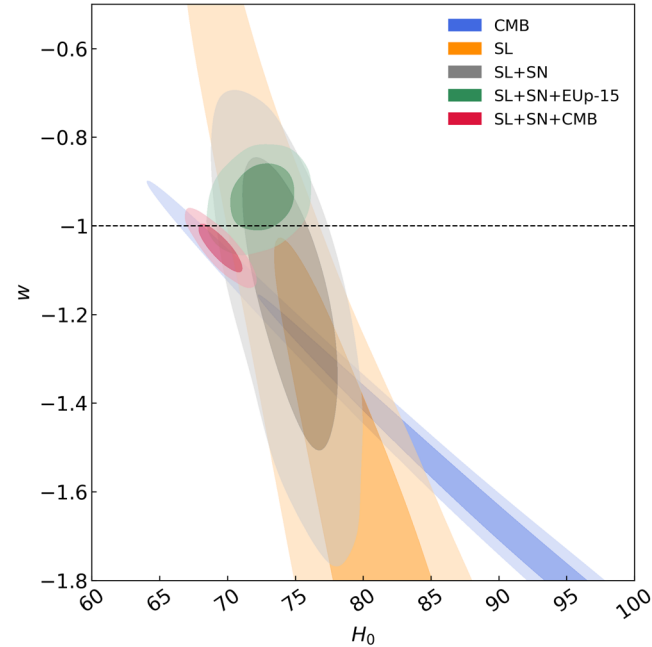


FIG. 3. Constraints from various dataset combinations within the w CDM model (H_0 has units of km/s Mpc⁻¹). Here the CMB data implies a complete analysis of the TT + TE + EE + low- l + lowE + lensing datasets for the w CDM model.

the w CDM framework. The H_0 -tension here is reduced to $\sim 2.2\sigma$ for both the CMB and CMB [high- l] priors, with a mildly phantomlike dark energy EOS. While we did not show the constraints on r_d here, we verify that they are in agreement with the expectation reported in Tables I and VII, when early Universe priors are included.

Through the parallel shift of the contours from CMB to CMB [high- l] priors as shown in Fig. 4, we notice that along the $w = -1$ parameter space, the constraints on the H_0 value are shifted towards higher values and with mildly larger uncertainty, which aids the supposition that with the exclusion of low- l likelihoods the tension can be moderately alleviated, however, not adequately alleviated. The constraint on the Hubble constant in the Λ CDM scenario shifts from $H_0 = 68.24^{+0.55}_{-0.61}$ km/s/Mpc⁻¹ to $H_0 = 68.97^{+0.77}_{-0.64}$ km/s/Mpc⁻¹, corresponding to $\sim 3.5\sigma$ and $\sim 2.8\sigma$ tension with respect to the H_0 estimate in R20, respectively.

At the same time, analysis with the inclusion of the EUp-15 allows for a larger range of possible H_0 values in agreement with the local R20 estimate and notably for the quintessence-like EOS $w > -1$, owing to the modified correlations in H_0 vs w parameter space (see also Fig. 3). Clearly, the observables through which the priors are implemented play a major role in determining the final correlations in the joint analysis. And this might even be a more appropriate analysis in comparison to the inclusion of the prior using the shift parameters, to assess the effects of excluding low- l + lowE likelihoods and combining the early CMB physics and late SN dynamics. Indeed, the distance priors in Eq. (4) also take into account the late-time behavior of the given model through the angular diameter distance $D_A(z^*)$. As shown in Fig. 4, simple exclusion of the low- l + lowE likelihoods shifts the constraints in the direction of the EUp-15/18 and further excluding the effects of late-time physics on the high- l part of the CMB spectrum moves the EUp-15/18 constraints, completely alleviating the H_0 -tension with the local R20

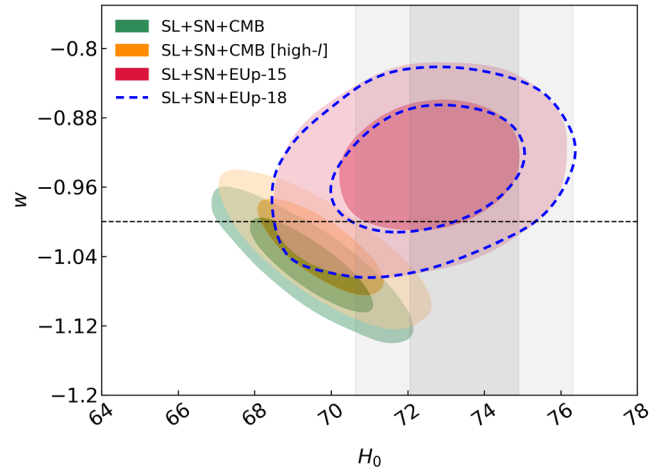


FIG. 4. We show the comparison between the final H_0 constraints for the three CMB priors used in the analyses. The gray band represents the local H_0 estimate of R18.

estimate. Both the EUp-15 and EUp-18 priors provide identical constraints and are in equally good agreement¹⁰ with the R20, where $H_0 = 72.5_{-1.6}^{+1.7}$ km/s/Mpc⁻¹. As shown in Fig. 7 (see also Table VII), the mild shift in the priors does not provide any visibly distinguishable effects in the joint analysis. This is clearly in accordance with the fact that the major improvements from the Planck 2015 to Planck 2018 likelihoods is within the modeling of the low- l and lowE likelihoods [27,136], essentially keeping the early Universe constraints unchanged. As shown in V17, the early Universe priors would remain unchanged when a $\Omega_k \neq 0$ ($k\Lambda$ CDM) freedom is taken into account, instead of the $w \neq -1$ freedom. This in turn asserts that our inferences here would be unaffected, even if the entire analysis is performed again using the $k\Lambda$ CDM model.

The $H_0 = 72.2 \pm 1.6$ km/s/Mpc⁻¹ constraint for the Λ CDM ($w = -1$) is also very much in agreement with the local R20 value. This tentatively indicates that the early Universe physics need not be modified while seeking a resolution to the H_0 -tension, and in turn the low- l likelihoods and the late-time effects on the high- l modeling of the CMB datasets could be appropriately revised. The H_0 -tension, which is usually assessed as a tension between the early physics constrained by CMB and late-time local estimate, we now recast as a disagreement between the late-time physics affecting the CMB analysis and the local estimate. As is elaborated in Refs. [75–78], the late-time cosmology effects enter the CMB analysis through the following: (i) the late integrated Sachs Wolfe effect (ISW), which affects the low- l ($l < 30$), (ii) suppression of the amplitude for $l \gg 40$, through the reionization effects, and (iii) an estimate of angular diameter distance [$D_A(z_{\text{rec}})$] to recombination, which in turn affects the angular scales.¹¹ This clearly implies that these three effects of the late-time physics on high- l CMB spectrum mark the difference between the constraints obtained utilizing the CMB [high- l] priors to the EUp-18/EUp-15 priors in our analysis. Finally, we also add the latest BAO dataset only to assert the variation in the inferred value of $H_0 = 68.98_{-0.80}^{+0.57}$ km/s/Mpc⁻¹ for the Λ CDM model, with the EUp-15 priors. This estimate is equivalent to using the CMB [high- l] priors without the BAO data, and might reflect the effect of assuming the low-redshift behavior through the fiducial cosmology, especially through the anisotropic

¹⁰Note that the constraint obtained from Hubble rate dataset, namely Cosmic Chromometers [131–134], which is $H_0 = 68.52_{-0.94}^{+0.94+2.51(\text{sys})}$ km/s/Mpc⁻¹ [135], will be in agreement with this estimate when accounting for the systematics.

¹¹The angular scale, i.e., location of the acoustic peaks in the CMB spectrum, essentially constrains the combination of the sound horizon [$r_s(z_{\text{rec}})$] and the angular diameter distance at the recombination, which are early-time and late-time physics dependent, respectively. The assumption of the same as fiducial cosmology in obtaining the BAO observables in turn makes them moderately dependent on late-time CMB physics, and might prevent the BAO data from being “truly” model independent.

component of BAO observables as elaborated in Ivanov *et al.* [93]. Excluding the BAO data from our main analysis and the final inferences is partly also due to the speculation of underestimated error bars in the traditional BAO analysis [90–92] and possible discordance with BAO data [85], which are mild and however require further validation.

Indeed, it is the physics of a low- l ($l \leq 30$) dataset within the CMB analysis, which is not yet very well understood, owing to the low- l anomalies [137,138], physics of reionization (polarization) [139,140], and the constraints from the ISW effect. For example in Refs. [141–144], it is claimed that some level of deviation forms the Λ CDM model in different physical scenarios. While we have not performed a low- l only analysis, the constraints, even in the current form, are instructive that low- l dataset alone would be inadequate to constrain cosmological models or at least in major disagreement with the other low-redshift probes like supernovae. Analyses and further progress in the direction of understanding the low- l physics could be thus promising.

It is also informative to contrast the early Universe constraints to the simple jackknifeline split of CMB data at $l \sim 800$, as shown in [27,63]. In the Λ CDM scenario, this split indicates that a lower value of H_0 (higher value of $\Omega_c h^2$) is preferred for $l > 800$ (with the TT,TE,EE dataset), indicating a mild discrepancy. This is removed when the lensing data is included (see Fig. 22 of [27]) and the constraints become consistent with $l < 800$ data, emphasizing the effect/impact of lensing data at higher multipoles. Also, when marginalizing on the lensing potential, V17 reports that excluding multipoles $l < 200$ provides highly degraded constraints, and will indicate no discrepancy. Indeed, the variation in constraints on $\Omega_c h^2$ (lower values from $l < 800$ and higher $l > 800$) would translate into a discrepancy between the H^{rec} estimates. This in turn would affect two distinct features: (i) silk damping at higher multipoles in the temperature and

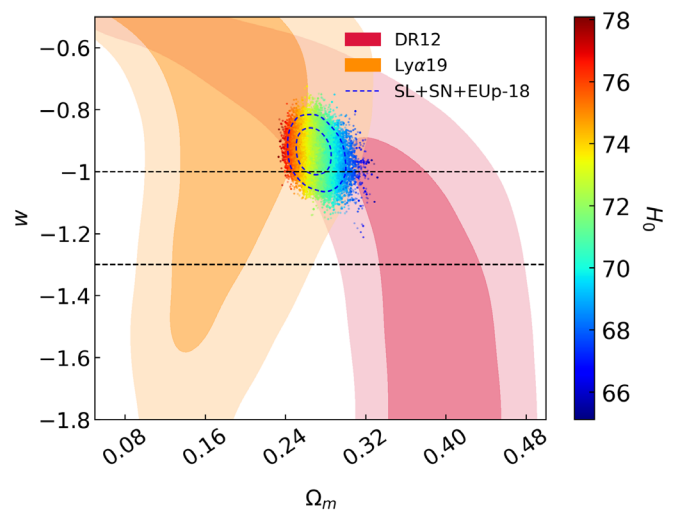


FIG. 5. Comparison of the Ω_m constraints obtained from the high-redshift Ly- α and the low-redshift galaxy clustering BAO DR12 datasets, for the w CDM model.

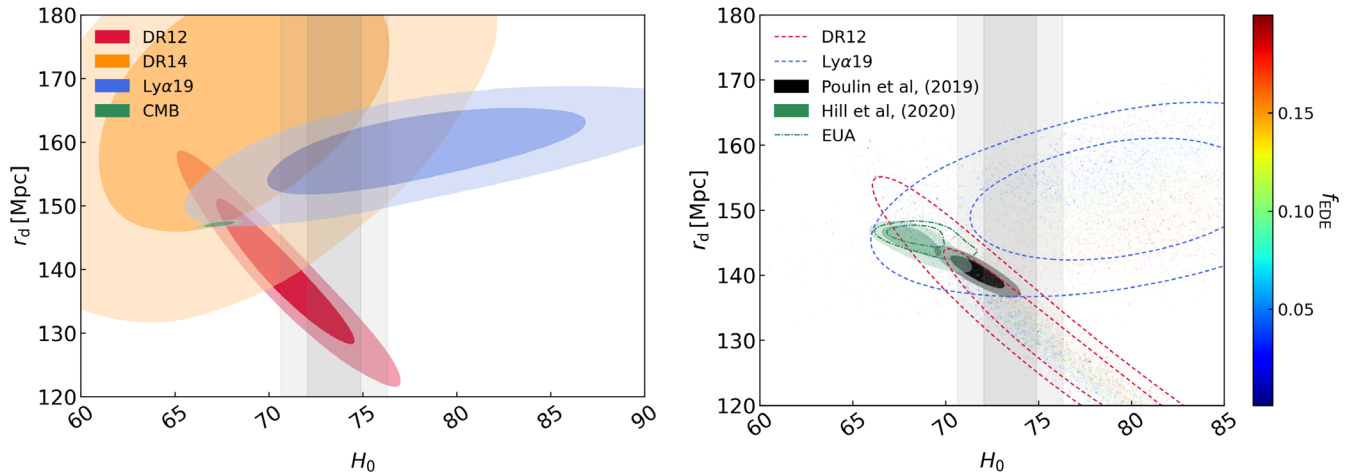


FIG. 6. Left: We show the comparison of inverse distance ladder analysis performed on different BAO datasets assuming the $\Omega_b h^2$ prior from CMB, as shown in Table I using the Λ CDM model. Here the CMB data implies complete analysis of the TT + TE + EE + low- l + lowE + lensing datasets for the Λ CDM model. Right: We show the EDE analysis with individual datasets, similar to the left panel. The EDE contours in *black* and *green* are the early dark energy constraints, corresponding to the $n = 3$ case presented in Table II of Poulin *et al.* [8] and Table II of Hill *et al.* [94] (CMB alone), respectively. The green dashed contours show our 3 pEDE constraints. Note that for brevity here we utilize the prior of $0.001 \leq f_{\text{EDE}} \leq 0.2$ for the BAO analysis, in contrast to the results quoted in the main text.

(ii) the polarization spectrum for the $l \lesssim 800$ explaining the discrepancy in the constraints on parameters such as $\{H_0, \Omega_c h^2\}$, when lensing data is not taken into account, in a $l \sim 800$ data split. Note that, when the lensing effects on the high l is taken into account (with or without marginalizing on the potential), the damping reduces making the constraints obtained using $l > 800$ + lensing consistent with those from $30 < l < 800$. However, this might also be in contention with the fact that the CMB anisotropies and the CMB-lensing data are at odds, observed as a $\sim 2\sigma$ deviation from unity for the parameter A_{Lens} [3,27,145,146]. See also [147], for various other data combinations, where the high- l ($l > 1000$) CMB TT and the TE, EE datasets are excluded, showing mild movement in the H_0 constraints for the Λ CDM model.

In Fig. 5, we show the comparison of the constraints in the w CDM model obtained for the Ly α 19 and the DR12 datasets. The constraints on the matter density from the high-redshift Ly α 19 and low-redshift DR12 datasets are clearly less compatible for $w < -1$, which limits possibilities of any phantomlike dark energy scenarios. Also, as the scatter of the H_0 values within the SL+SN+EUp-18 shows, the high-redshift Ly α 19 is yet compatible with a $w \sim -1$ and larger values of H_0 , which is not the case with the DR12 data. Including the Ly α 19 and DR12 datasets separately to the SL+SN+EUp-18 fits, we obtain $H_0 = 72.03^{+1.55}_{-1.59}$ km/s/Mpc $^{-1}$ and $H_0 = 69.04 \pm 0.83$ km/s/Mpc $^{-1}$, respectively. In this respect, one could disentangle the data corresponding to the late-time physics in CMB data and the low-redshift BAO clustering DR12 datasets as the cosmological data which is incompatible with the local H_0 R20 estimate. Recently, in [148], the constraints in the w CDM scenario have been explored with various combinations of datasets.

In the left panel of Fig. 6 we show the comparison of the inverse distance ladder analysis performed on the different BAO datasets for the Λ CDM model. We notice the orthogonal nature of the correlations of the r_d vs H_0 parameters derived from the Ly α 19 and DR12 combinations, which is a known behavior and has been presented earlier (see, for example, [84]). However, this orthogonality implies that the usual early Universe modifications, intended to reduce the sound horizon at drag epoch and hence accommodate a larger values of H_0 , will clearly be in agreement with the DR12 dataset.¹² And the already existing 2.3σ tension¹³ [107,108] could possibly become worse or at best remain at a similar significance, and cannot necessarily be seen as a simple statistical fluke or systematic effects in the Ly α 19 dataset. This orthogonality of constraints in the r_d vs H_0 between the DR12 and Ly α 19 datasets might in fact suggests that an early Universe modification alone cannot alleviate the H_0 -tension and some late-time modification is also required. Also note the redshift dependent behavior of the change in the r_d vs H_0 from the DR12 ($0.2 < z < 0.75$), to the DR14 ($0.8 < z < 2.2$) and the Ly α 19 ($1.77 < z < 3.5$) datasets. This redshift dependent behavior could be of the utmost importance also with the soon to be available DR16 [149–151] datasets, which we intend to explore elsewhere [152].

¹²The early dark energy modifications in Poulin *et al.* [8] modify the prerecombination calibration of r_d as a function of the matter densities allowing for larger parameter space in r_d vs H_0 parameter space.

¹³This tension has now been reduced to 1.5σ in the latest DR16 release [149]. However, the correlation between r_d vs H_0 parameters is bound to be the same and hence the argument for the alleviated H_0 -tension.

We also compare the constraints in the r_d vs H_0 plane for the EDE analysis presented in [8], which was shown to alleviate the H_0 -tension. However, more recently [94] has argued that there is no evidence for EDE when using CMB data alone, owing to minimal improvement in the $\Delta\chi^2 \sim -4.1$ with an inclusion of 3 additional parameters, and the improvement in the χ^2 is mostly contributed by the inclusion of local H_0 value. In [79] it has been shown that the EDE models will increase the discrepancy with the large scale structure data, owing to the tension in the σ_8 parameter. This, in fact, aids the motivation for the arguments raised in the current work. In Ref. [101], it has been shown that accounting for the large unconstrained distributions of $\{\log_{10}(z_c), \theta_i\}$ parameters can alleviate the above mentioned issues, having only one additional parameter.

To estimate the effect of the EDE extension on the BAO constraints, we perform a similar analysis with different BAO datasets for the EDE model. We fix the EDE parameters $\{\log_{10}(z_c), \theta_i\}$ as in the analysis presented in Smith *et al.* [101] to the best-fit values reported in Table II of Hill *et al.* [94], varying only $\{\omega_{\text{cdm}}, H_0, f_{\text{EDE}}\}$. As expected, we find the contours in the r_d vs H_0 plane extend to the higher values of H_0 and lower values of r_d for both the DR12 and the Ly α 19 datasets. However, marginalizing on the $f_{\text{EDE}} \in \{0.001, 0.5\}$, we find that the mild to moderate disagreement between the DR12 and Ly α 19 datasets remains as $\Omega_m = 0.384^{+0.055}_{-0.062}$ and $\Omega_m = 0.198^{+0.034}_{-0.055}$, respectively. This disagreement is at a tentative tension of $\sim 2.7\sigma$ significance. When including the local R18 prior to the joint analysis of DR14 and Ly α 19 we find the constraint $f_{\text{EDE}} = 0.189^{+0.065}_{-0.054}$. We present the complete contours for the parameters of the analysis of BAO datasets in Appendix B. Conveniently, we also verify that these results agree with the Λ CDM analysis for $f_{\text{EDE}} = 0$ and accordingly are seen for $w = -1$ in Fig. 5.

V. CONCLUSIONS

In the current work, we attempt to assess the origins (necessary and sufficient modifications of physical models) of the H_0 -tension within the CMB likelihoods, essentially distinguishing the early-time and late-time physics. We implement this through a very simple joint analysis, utilizing the CMB data in various reduced forms as priors. A summary of our primary inferences is as follows:

- (i) We find that the exclusion of the low- l + lowE likelihoods from the CMB analysis relaxes the phantom-like constraints on the dark energy EOS and is thus able to raise the value of high-redshift H_0 towards larger values being consistent with $w \rightarrow -1$. However, in conjunction with the well-constrained dynamics at low redshift by the SNe dataset, we find it highly unlikely to be sufficient to resolve the H_0 -tension.
- (ii) Using early Universe priors from CMB data (EUp-15/18) which disentangle the late-time and

early-time physics (see also [75,77,78]), we find that the early-time physics can indeed be consistent with a local estimate of H_0 , within the Λ CDM model when excluding the galaxy-clustering BAO DR12 dataset.

- (iii) We analyze the EDE model using the EUA of the CMB data finding no evidence for the EDE extension with $f_{\text{EDE}} < 0.07$ at 95% C.L. limits, which is sufficient to alleviate the H_0 -tension. In the 1 pEDE analysis this constraint is relaxed to $f_{\text{EDE}} < 0.08$.
- (iv) Through our simple EUA of EDE model and due to the fact that the high- l fit worsens when alleviating the H_0 -tension in EDE model, we speculate that modifications in the physics or systematics effects might be required in the CMB low- l modeling and/or late-time physics. Clearly, the analysis performed here is not sufficient to point to the actual needed physics or to the systematics, but overall implies that the late-times physics within the CMB data might be responsible for the tension.
- (v) The orthogonality of the DR12 and Ly α 19 dataset constraints in the r_d vs H_0 parameter space suggests that an early Universe modification alone cannot be sufficient to resolve the H_0 -tension. At least a combination of both late and early Universe modifications would be required.

The inferences here, if taken at face value, recast the usual perspective of the H_0 -tension as an early-time CMB vs local (late-time) physics effect to a late-time physics in CMB vs local perspective. In light of recent high precision data, the increasing H_0 -tension is a pressing issue for the current cosmological scenario, making it very important to be resolved as soon as possible in the near future. While newer and more precise data will aid the cause, it is vital to pinpoint the origins of the tension and find appropriate directions to drive the numerous efforts taken in the theoretical modeling and in the estimates of systematic and statistical errors.

ACKNOWLEDGMENTS

B. S. H. and N. V. acknowledge financial support by ASI Grant No. 2016-24-H.0. M. V is supported by INFN INDARK PD51 grant and agreement Agenzia Spaziale Italiana-Istituto nazionale di astrofisica (ASI-INAF) No. 2017-14-H.0. B. S. H acknowledges Istituto nazionale di fisica nucleare (INFN) Roma, Tor Vergata Computing Center services (RMLab) and is thankful to Federico Zani for providing assistance. We acknowledge the use of CINECA high performance computing resources under the projects “INF19_indark_0” and “INF20_indark”. We are grateful to Nils Schöneberg for very useful clarifications on the CLASS and CAMB comparison. We thank the authors of Verde *et al.* [75] for providing us the covariances of the EUp-15 used in this work. The authors are grateful to Vivian Poulin and Riccardo Murgia for useful comments on the draft and providing us with information from their work

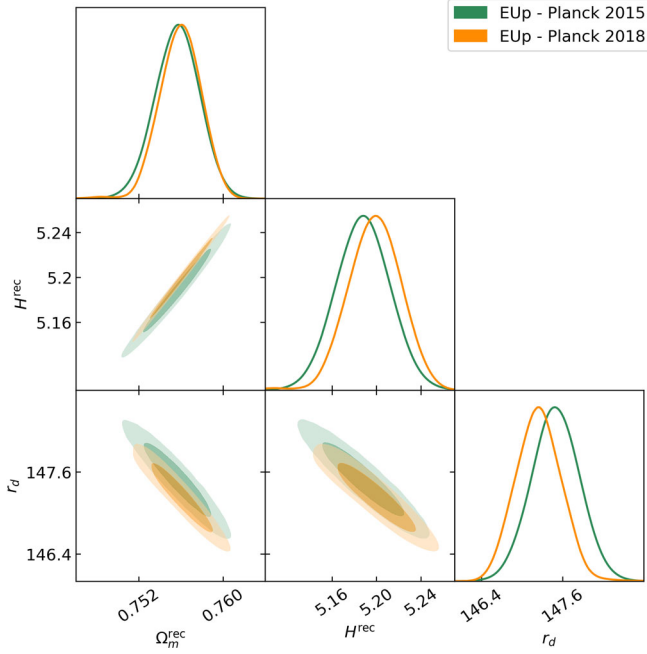


FIG. 7. Comparison of the early Universe constraints between the Planck 2015, Verde *et al.* [75] analysis and our analysis with Planck 2018 likelihoods. H^{rec} and r_d are reported in Mpc^{-1} and Mpc , respectively.

Poulin *et al.* [8]. We thank Bohdan Bidenko for assistance with ΛCDM analysis of the BAO data.

APPENDIX A: CMB PRIORS

In this section we first report the covariances matrices of distance priors used in the analysis, which reproduce the joint analyses. As it has been earlier asserted in [73,74], we find the distance priors sufficiently capable of replacing the complete CMB data analysis. We perform simple importance sampling¹⁴ analysis to validate the same.

In Fig. 7, we contrast the constraints on the early Universe quantities as were reported in Verde *et al.* [75] with the analysis replicated here using the Planck 2018 likelihoods. We find a very mild shift in the quantities mostly being consistent with the earlier results. The corresponding covariances for the Planck 2018 are reported in Table VII and can be compared against Table I, presented in Sec. III. This small shift in the constraints is in accordance with the difference in the physical densities estimated from Planck 2015 [72] to Planck 2018 [27]. Note that we have not validated the agreement of the EUp-18 across the ΛCDM and $k\Lambda\text{CDM}$ models, as reported in V17; however, we expect it to remain, owing to the minimal variation in the 2015 and 2018 Planck likelihoods.

¹⁴We use the ChainConsumer [153] package to perform the importance sampling validation. The code is publicly available at [154].

TABLE V. Mean values and the corresponding covariances of the distance priors for the complete CMB (TT, TE, EE + low- l + lowE + lensing) dataset. Here $z_* = 1089.79 \pm 0.26$.

| Observable | Mean | σ_i | r_{ij} | | |
|--------------------|--------|------------|----------|-------|-------|
| $R(z_*)$ | 1.7477 | 0.0041 | 1. | 0.44 | -0.65 |
| $l_A(z_*)$ | 301.74 | 0.08 | 0.44 | 1. | -0.33 |
| $10^2\Omega_b h^2$ | 2.243 | 0.015 | -0.65 | -0.33 | 1. |

TABLE VI. Same as Table V, excluding the low- l + lowE datasets (i.e., CMB [high- l]). Here $z_* = 1089.69 \pm 0.31$.

| Observable | Mean | σ_i | r_{ij} | | |
|--------------------|--------|------------|----------|-------|-------|
| $R(z_*)$ | 1.7418 | 0.0053 | 1. | 0.48 | -0.72 |
| $l_A(z_*)$ | 301.68 | 0.09 | 0.48 | 1. | -0.37 |
| $10^2\Omega_b h^2$ | 2.247 | 0.016 | -0.72 | -0.37 | 1. |

TABLE VII. Mean values and the corresponding covariances of the EUp-18. H^{rec} and r_d are reported in Mpc^{-1} and Mpc , respectively.

| Observable | Mean | σ_i | r_{ij} | | | |
|--------------------|--------|-----------------------|----------|-------|-------|-------|
| $10^2\Omega_b h^2$ | 2.246 | 1.60×10^{-2} | 1. | -0.73 | -0.71 | 0.39 |
| $10^2\Omega_c h^2$ | 11.90 | 1.70×10^{-1} | -0.73 | 1. | 0.99 | -0.91 |
| H^{rec} | 5.198 | 2.40×10^{-2} | -0.71 | 0.99 | 1. | -0.92 |
| r_d | 147.24 | 0.34 | 0.39 | -0.91 | -0.92 | 1. |

APPENDIX B: BAO CONSTRAINTS ON THE EDE MODEL

In this section we present the complete constraints for the EDE model. The analysis is performed through the 1 pEDE formalism presented in Smith *et al.* [101]. As expected, we do not find any constraints on the f_{EDE} using the individual BAO datasets, and even in the joint analysis. However, also interesting to note is that the parameter tends towards larger values in contrast to the lower values preferred from the CMB data. While the σ_8 parameter is not necessarily constrained by the BAO datasets, the disagreement is induced especially by the Ω_m limits. In Fig. 8, we show the constraint for the EDE model using the individual datasets and the joint analysis. More importantly, with the inclusion of the R18¹⁵ in the analysis we find the limits of $f_{\text{EDE}} = 0.189^{+0.065}_{-0.054}$ (neglecting the disagreement in the BAO datasets for the moment). As we follow the 1 pEDE formalism of Smith *et al.* [101], we can immediately see that our limits are in very good agreement with the constraints presented therein.

¹⁵Note that here we have utilized R18, instead of the more recent R20, which, however, does not make any difference to the relevant conclusions here.

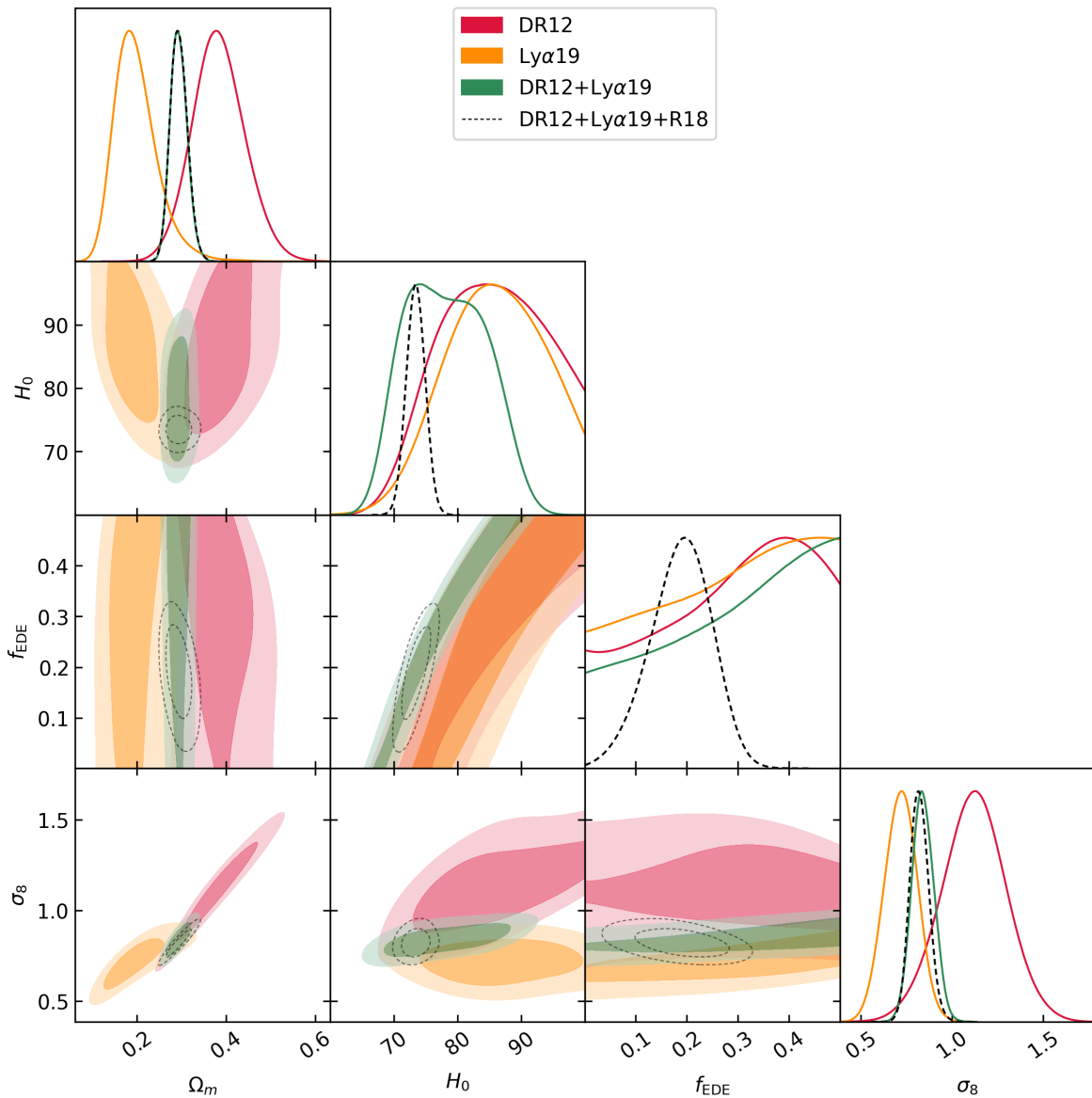


FIG. 8. We present the 68% and 95% C.L. contours for the EDE constraints obtained from the individual BAO datasets and their joint analysis.

-
- [1] K. C. Wong *et al.*, *Mon. Not. R. Astron. Soc.* **498**, 1420 (2020).
 [2] A. G. Riess, *Nat. Rev. Phys.* **2**, 10 (2020).
 [3] L. Verde, T. Treu, and A. G. Riess, *Nat. Astron.* **3**, 891 (2019).
 [4] E. Di Valentino *et al.*, [arXiv:2008.11284](https://arxiv.org/abs/2008.11284).
 [5] E. Di Valentino, *Mon. Not. Roy. Astron. Soc.* **502**, 2065 (2021).
 [6] N. Khosravi and S. Baghran, *Phys. Rev. D* **99**, 103526 (2019).
 [7] A. Banihashemi, N. Khosravi, and A. H. Shirazi, *Phys. Rev. D* **99**, 083509 (2019).
 [8] V. Poulin, T. L. Smith, T. Karwal, and M. Kamionkowski, *Phys. Rev. Lett.* **122**, 221301 (2019).
 [9] T. Karwal and M. Kamionkowski, *Phys. Rev. D* **94**, 103523 (2016).
 [10] J.-Q. Xia and M. Viel, *J. Cosmol. Astropart. Phys.* **09** (2009) 002.
 [11] G. Ye and Y.-S. Piao, *Phys. Rev. D* **101**, 083507 (2020).
 [12] G. Ye and Y.-S. Piao, *Phys. Rev. D* **102**, 083523 (2020).

- [13] E. Mortsell and S. Dhawan, *J. Cosmol. Astropart. Phys.* **09** (2018) 025.
- [14] A. Gogoi, P. Chanda, and S. Das, [arXiv:2005.11889](https://arxiv.org/abs/2005.11889).
- [15] J. Sakstein and M. Trodden, *Phys. Rev. Lett.* **124**, 161301 (2020).
- [16] H. Khoraminezhad, M. Viel, C. Baccigalupi, and M. Archidiacono, *J. Cosmol. Astropart. Phys.* **07** (2020) 039.
- [17] W. Yang, S. Pan, E. Di Valentino, R. C. Nunes, S. Vagnozzi, and D. F. Mota, *J. Cosmol. Astropart. Phys.* **09** (2018) 019.
- [18] S. Pan, W. Yang, E. Di Valentino, E. N. Saridakis, and S. Chakraborty, *Phys. Rev. D* **100**, 103520 (2019).
- [19] E. Di Valentino, A. Melchiorri, and O. Mena, *Phys. Rev. D* **96**, 043503 (2017).
- [20] A. Hryczuk and K. Jodłowski, *Phys. Rev. D* **102**, 043024 (2020).
- [21] M. Archidiacono, D. C. Hooper, R. Murgia, S. Bohr, J. Lesgourgues, and M. Viel, *J. Cosmol. Astropart. Phys.* **10** (2019) 055.
- [22] M. Braglia, M. Ballardini, F. Finelli, and K. Koyama, *Phys. Rev. D* **103**, 043528 (2021).
- [23] T. L. Smith, V. Poulin, and M. A. Amin, *Phys. Rev. D* **101**, 063523 (2020).
- [24] M.-X. Lin, G. Benevento, W. Hu, and M. Raveri, *Phys. Rev. D* **100**, 063542 (2019).
- [25] P. Agrawal, F.-Y. Cyr-Racine, D. Pinner, and L. Randall, [arXiv:1904.01016](https://arxiv.org/abs/1904.01016).
- [26] M.-X. Lin, W. Hu, and M. Raveri, *Phys. Rev. D* **102**, 123523 (2020).
- [27] N. Aghanim *et al.* (Planck Collaboration), *Astron. Astrophys.* **641**, A6 (2020).
- [28] G. Blackadder and S. M. Koushiappas, *Phys. Rev. D* **90**, 103527 (2014).
- [29] K. Vattis, S. M. Koushiappas, and A. Loeb, *Phys. Rev. D* **99**, 121302 (2019).
- [30] G. Choi, M. Suzuki, and T. T. Yanagida, *Phys. Lett. B* **805**, 135408 (2020).
- [31] V. Poulin, P. D. Serpico, and J. Lesgourgues, *J. Cosmol. Astropart. Phys.* **08** (2016) 036.
- [32] B. S. Haridasu and M. Viel, *Mon. Not. R. Astron. Soc.* **497**, 1757 (2020).
- [33] G. F. Abellan, R. Murgia, V. Poulin, and J. Lavalley, [arXiv:2008.09615](https://arxiv.org/abs/2008.09615).
- [34] S. J. Clark, K. Vattis, and S. M. Koushiappas, *Phys. Rev. D* **103**, 043014 (2021).
- [35] M. Raveri, *Phys. Rev. D* **101**, 083524 (2020).
- [36] L. Verde, J. L. Bernal, A. F. Heavens, and R. Jimenez, *Mon. Not. R. Astron. Soc.* **467**, 731 (2017).
- [37] V. Poulin, K. K. Boddy, S. Bird, and M. Kamionkowski, *Phys. Rev. D* **97**, 123504 (2018).
- [38] K. Aylor, M. Joy, L. Knox, M. Millea, S. Raghunathan, and W. K. Wu, *Astrophys. J.* **874**, 4 (2019).
- [39] P. Lemos, E. Lee, G. Efstathiou, and S. Gratton, *Mon. Not. R. Astron. Soc.* **483**, 4803 (2019).
- [40] N. Arendse, A. Agnello, and R. J. Wojtak, *Astron. Astrophys.* **632**, A91 (2019).
- [41] M.-Z. Lyu, B. S. Haridasu, M. Viel, and J.-Q. Xia, *Astrophys. J.* **900**, 160 (2020).
- [42] R. C. Keenan, A. J. Barger, and L. L. Cowie, *Astrophys. J.* **775**, 62 (2013).
- [43] T. Shanks, L. M. Hogarth, and N. Metcalfe, *Mon. Not. R. Astron. Soc.* **484**, L64 (2019).
- [44] B. L. Hoscheit and A. J. Barger, *Astrophys. J.* **854** 46 (2018).
- [45] N. Schöneberg, J. Lesgourgues, and D. C. Hooper, *J. Cosmol. Astropart. Phys.* **10** (2019) 029.
- [46] W. D. Kenworthy, D. Scolnic, and A. Riess, *Astrophys. J.* **875**, 145 (2019).
- [47] V. V. Luković, B. S. Haridasu, and N. Vittorio, *Mon. Not. R. Astron. Soc.* **2671**, 2075 (2019).
- [48] R.-G. Cai, J.-F. Ding, Z.-K. Guo, S.-J. Wang, and W.-W. Yu, [arXiv:2012.08292](https://arxiv.org/abs/2012.08292).
- [49] S. Birrer *et al.*, *Mon. Not. R. Astron. Soc.* **484**, 4726 (2019).
- [50] M. Millon *et al.*, *Astron. Astrophys.* **639**, A101 (2020).
- [51] S. Birrer *et al.*, *Astron. Astrophys.* **643**, A165 (2020).
- [52] L. Knox and M. Millea, *Phys. Rev. D* **101**, 043533 (2020).
- [53] N. Arendse *et al.*, *Astron. Astrophys.* **639**, A57 (2020).
- [54] M. Raveri and W. Hu, *Phys. Rev. D* **99**, 043506 (2019).
- [55] K. Jedamzik, L. Pogosian, and G.-B. Zhao, [arXiv:2010.04158](https://arxiv.org/abs/2010.04158).
- [56] W. L. K. Wu, P. Motloch, and W. Hu, and M. Raveri, *Phys. Rev. D* **102**, 023510 (2020).
- [57] M. M. Ivanov, Y. Ali-Haïmoud, and J. Lesgourgues, *Phys. Rev. D* **102**, 063515 (2020).
- [58] J. L. Bernal, T. L. Smith, K. K. Boddy, and M. Kamionkowski, *Phys. Rev. D* **102**, 123515 (2020).
- [59] E. Di Valentino, A. Melchiorri, E. V. Linder, and J. Silk, *Phys. Rev. D* **96**, 023523 (2017).
- [60] S. Vagnozzi, *Phys. Rev. D* **102**, 023518 (2020).
- [61] G. Alestas, L. Kazantzidis, and L. Perivolaropoulos, *Phys. Rev. D* **101**, 123516 (2020).
- [62] W. Handley, *Phys. Rev. D* **103**, L041301 (2021).
- [63] E. Di Valentino, A. Melchiorri, and J. Silk, *Nat. Astron.*, [arXiv:1911.02087](https://arxiv.org/abs/1911.02087).
- [64] D. M. Scolnic *et al.*, *Astrophys. J.* **859**, 101 (2018).
- [65] S. Taubenberger, S. H. Suyu, E. Komatsu, I. Jee, S. Birrer, V. Bonvin, F. Courbin, C. E. Rusu, A. J. Shajib, and K. C. Wong, *Astron. Astrophys.* **628**, L7 (2019).
- [66] A. G. Riess *et al.*, *Astrophys. J.* **855**, 136 (2018).
- [67] A. G. Riess, S. Casertano, W. Yuan, L. M. Macri, and D. Scolnic, *Astrophys. J.* **876**, 85 (2019).
- [68] A. G. Riess, S. Casertano, W. Yuan, J. B. Bowers, L. Macri, J. C. Zinn, and D. Scolnic, *Astrophys. J. Lett.* **908**, L6 (2021).
- [69] Y. Wang and P. Mukherjee, *Astrophys. J.* **650**, 1 (2006).
- [70] Y. Wang and P. Mukherjee, *Phys. Rev. D* **76**, 103533 (2007).
- [71] E. Komatsu *et al.* (WMAP Collaboration), *Astrophys. J. Suppl.* **180**, 330 (2009).
- [72] P. A. R. Ade *et al.* (Planck Collaboration), *Astron. Astrophys.* **594**, A14 (2016).
- [73] L. Chen, Q.-G. Huang, and K. Wang, *J. Cosmol. Astropart. Phys.* **02** (2019) 028.
- [74] Z. Zhai, C.-G. Park, Y. Wang, and B. Ratra, *J. Cosmol. Astropart. Phys.* **07** (2020) 009.
- [75] L. Verde, E. Bellini, C. Pigozzo, A. F. Heavens, and R. Jimenez, *J. Cosmol. Astropart. Phys.* **04** (2017) 023.

- [76] M. Vonlanthen, S. Rsnen, and R. Durrer, *J. Cosmol. Astropart. Phys.* **08** (2010) 023.
- [77] B. Audren, J. Lesgourgues, K. Benabed, and S. Prunet, *J. Cosmol. Astropart. Phys.* **02** (2013) 001.
- [78] B. Audren, *Mon. Not. R. Astron. Soc.* **444**, 827 (2014).
- [79] M. M. Ivanov, E. McDonough, J. C. Hill, M. Simonović, M. W. Toomey, S. Alexander, and M. Zaldarriaga, *Phys. Rev. D* **102**, 103502 (2020).
- [80] D. J. Eisenstein *et al.* (SDSS Collaboration), *Astrophys. J.* **633**, 560 (2005).
- [81] S. Alam *et al.* (BOSS Collaboration), *Mon. Not. R. Astron. Soc.* **470**, 2617 (2017).
- [82] J. E. Bautista *et al.*, *Astron. Astrophys.* **603**, A12 (2017).
- [83] H. du Mas des Bourboux *et al.*, *Astron. Astrophys.* **608**, A130 (2017).
- [84] É. Aubourg *et al.*, *Phys. Rev. D* **92**, 123516 (2015).
- [85] B. S. Haridasu, V. V. Luković, and N. Vittorio, *J. Cosmol. Astropart. Phys.* **05** (2018) 033.
- [86] J. L. Bernal, L. Verde, and A. G. Riess, *J. Cosmol. Astropart. Phys.* **10** (2016) 019.
- [87] C.-G. Park and B. Ratra, *Astrophys. Space Sci.* **364**, 82 (2019).
- [88] A. J. Cuesta, L. Verde, A. Riess, and R. Jimenez, *Mon. Not. R. Astron. Soc.* **448**, 3463 (2015).
- [89] D. Camarena and V. Marra, *Mon. Not. R. Astron. Soc.* **495**, 2630 (2020).
- [90] S. Anselmi, P.-S. Corasaniti, A. G. Sanchez, G. D. Starkman, R. K. Sheth, and I. Zehavi, *Phys. Rev. D* **99**, 123515 (2019).
- [91] S. Anselmi, G. D. Starkman, P.-S. Corasaniti, R. K. Sheth, and I. Zehavi, *Phys. Rev. Lett.* **121**, 021302 (2018).
- [92] S. Anselmi, P.-S. Corasaniti, G. D. Starkman, R. K. Sheth, and I. Zehavi, *Phys. Rev. D* **98**, 023527 (2018).
- [93] M. M. Ivanov, M. Simonović, and M. Zaldarriaga, *J. Cosmol. Astropart. Phys.* **05** (2020) 042.
- [94] J. C. Hill, E. McDonough, M. W. Toomey, and S. Alexander, *Phys. Rev. D* **102**, 043507 (2020).
- [95] G. D'Amico, L. Senatore, P. Zhang, and H. Zheng, *arXiv:2006.12420*.
- [96] M. Lucca, *Phys. Lett. B* **810**, 135791 (2020).
- [97] T. Abbott *et al.* (DES Collaboration), *Phys. Rev. D* **98**, 043526 (2018).
- [98] H. Hildebrandt *et al.*, *Mon. Not. R. Astron. Soc.* **465**, 1454 (2017).
- [99] H. Hildebrandt *et al.*, *Astron. Astrophys.* **633**, A69 (2020).
- [100] C. Hikage *et al.* (HSC Collaboration), *Publ. Astron. Soc. Jpn.* **71**, 43 (2019).
- [101] T. L. Smith, V. Poulin, J. L. Bernal, K. K. Boddy, M. Kamionkowski, and R. Murgia, *arXiv:2009.10740*.
- [102] F. Niedermann and M. S. Sloth, *arXiv:2009.00006*.
- [103] A. Chudaykin, D. Gorbunov, and N. Nedelko, *Phys. Rev. D* **103**, 043529 (2021).
- [104] D. J. Fixsen, *Astrophys. J.* **707**, 916 (2009).
- [105] https://github.com/mwt5345/class_edu
- [106] G.-B. Zhao *et al.*, *Mon. Not. R. Astron. Soc.* **482**, 3497 (2019).
- [107] M. Blomqvist, H. du Mas des Bourboux *et al.*, *Astron. Astrophys.* **629**, A86 (2019).
- [108] V. de Sainte Agathe, C. Balland *et al.*, *Astron. Astrophys.* **629**, A85 (2019).
- [109] W. Hu and N. Sugiyama, *Astrophys. J.* **471**, 542 (1996).
- [110] https://github.com/brinckmann/montepython_public
- [111] T. Brinckmann and J. Lesgourgues, *Phys. Dark Universe* **24**, 100260 (2019).
- [112] <http://dfm.io/emcee/current/>
- [113] D. Foreman-Mackey, D. W. Hogg, D. Lang, and J. Goodman, *Publ. Astron. Soc. Pac.* **125**, 306 (2013).
- [114] <https://getdist.readthedocs.io/>
- [115] A. Lewis, *arXiv:1910.13970*.
- [116] <https://camb.readthedocs.io/en/latest/>
- [117] A. Lewis and S. Bridle, *Phys. Rev. D* **66**, 103511 (2002).
- [118] A. Lewis and A. Challinor, CAMB: Code for Anisotropies in the Microwave Background, 2011, ascl:1102.026.
- [119] https://github.com/lesgourg/class_public
- [120] J. Lesgourgues, *arXiv:1104.2932*.
- [121] D. Blas, J. Lesgourgues, and T. Tram, *J. Cosmol. Astropart. Phys.* **07** (2011) 034.
- [122] J. Lesgourgues, *arXiv:1104.2934*.
- [123] A. Gelman and D. B. Rubin, *Stat. Sci.* **7**, 457 (1992).
- [124] L. Pagano, J. M. Delouis, S. Mottet, J. L. Puget, and L. Vibert, *Astron. Astrophys.* **635**, A99 (2020).
- [125] R. Murgia, G. F. Abellán, and V. Poulin, *arXiv:2009.10733* [Phys. Rev. D (to be published)].
- [126] H. Hildebrandt *et al.*, *Astron. Astrophys.* **633**, A69 (2020).
- [127] S. Joudaki *et al.*, *Astron. Astrophys.* **638**, L1 (2020).
- [128] M. Asgari *et al.* (KiDS Collaboration), *Astron. Astrophys.* **645**, A104 (2021).
- [129] C. Heymans, T. Tröster, M. Asgari, C. Blake, H. Hildebrandt, and B. Joachimi *et al.*, *Astron. Astrophys.* **646**, A140 (2021).
- [130] E. Di Valentino *et al.*, *arXiv:2008.11285*.
- [131] R. Jimenez and A. Loeb, *Astrophys. J.* **573**, 37 (2002).
- [132] M. Moresco *et al.*, *J. Cosmol. Astropart. Phys.* **08** (2012) 006.
- [133] M. Moresco, *Mon. Not. R. Astron. Soc.* **450**, L16 (2015).
- [134] M. Moresco, L. Pozzetti, A. Cimatti, R. Jimenez, C. Maraston, L. Verde, D. Thomas, A. Citro, R. Tojeiro, and D. Wilkinson, *J. Cosmol. Astropart. Phys.* **05** (2016) 014.
- [135] B. S. Haridasu, V. V. Luković, M. Moresco, and N. Vittorio, *J. Cosmol. Astropart. Phys.* **10** (2018) 015.
- [136] N. Aghanim *et al.* (Planck Collaboration), *Astron. Astrophys.* **596**, A107 (2016).
- [137] A. Rassat, J. L. Starck, P. Paykari, F. Sureau, and J. Bobin, *J. Cosmol. Astropart. Phys.* **08** (2014) 006.
- [138] D. J. Schwarz, C. J. Copi, D. Huterer, and G. D. Starkman, *Classical Quantum Gravity* **33**, 184001 (2016).
- [139] M. Billi, A. Gruppuso, N. Mandolesi, L. Moscardini, and P. Natoli, *Phys. Dark Universe* **26**, 100327 (2019).
- [140] G. Obied, C. Dvorkin, C. Heinrich, W. Hu, and V. Miranda, *Phys. Rev. D* **96**, 083526 (2017).
- [141] S. Das, A. Shafieloo, and T. Souradeep, *J. Cosmol. Astropart. Phys.* **10** (2013) 016.
- [142] H. Velten, H. A. Borges, S. Carneiro, R. Fazolo, and S. Gomes, *Mon. Not. R. Astron. Soc.* **452**, 2220 (2015).
- [143] B. Mostaghel, H. Moshafi, and S. M. S. Movahed, *Mon. Not. R. Astron. Soc.* **481**, 1799 (2018).
- [144] A. M. Soltan, *Mon. Not. R. Astron. Soc.* **488**, 2732 (2019).
- [145] F. Renzi, E. Di Valentino, and A. Melchiorri, *Phys. Rev. D* **97**, 123534 (2018).

-
- [146] E. Di Valentino and S. Bridle, *Symmetry* **10**, 585 (2018).
[147] A. Chudaykin, D. Gorbunov, and N. Nedelko, *J. Cosmol. Astropart. Phys.* **08** (2020) 013.
[148] G. D'Amico, Y. Donath, L. Senatore, and P. Zhang, [arXiv:2012.07554](https://arxiv.org/abs/2012.07554).
[149] H. du Mas des Bourboux *et al.*, *Astrophys. J.* **901**, 153 (2020).
[150] J. Hou *et al.*, *Mon. Not. R. Astron. Soc.* **500**, 1201 (2020).
[151] J. E. Bautista *et al.*, *Mon. Not. R. Astron. Soc.* **500**, 736 (2020).
[152] B. Bidenko *et al.* (to be published).
[153] S. R. Hinton, *J. Open Source Softw.* **1**, 00045 (2016).
[154] <https://github.com/Samreay/ChainConsumer/tree/Final-Paper>